CEBAF Program Advisory Committee Eight Cover Sheet

This proposal must be received by close of business on Thursday, April 14, 1994 at:

CEBAF
User Liaison Office, Mail Stop 12 B
12000 Jefferson Avenue
Newport News, VA 23606

Proposal Title

Longitudinal and Transverse Cross Sections in the $d(e,e'K^{+})YN$ Rreactions at $Q^2 = 0.5$ to $2\ (\mathrm{GeV}/c)^2$

Contact Person

Name: Shelton Y. Beedoe

Institution: Hampton University

Address: Department of Physics, Hampton University

Address:

City, State ZIP/Country: Hampton, VA 23668

Phone: (804)727-5951 or 249-7168 **FAX:** (804)727-5955 or 249-7363

E-Mail → Internet: BEEDOE@cebaf.gov

Experimental Hall: C

Total Days Requested for Approval: 22

Minimum and Maximum Beam Energies (GeV): 2.4 & 4.0

Minimum and Maximum Beam Currents (μAmps): 10 & 30

CEBAF Use Only

Receipt Date: ______________________

By: ______________________

HAZARD IDENTIFICATION CHECKLIST

CEBAF Experiment: 94-009 Date: 5/25/94

Check all items for which there is an anticipated need—do not check items that are part of the CEBAF standard experiment (HRSE, HRSH, CLAS, HMS, SOS in standard configurations).

Cryogenics	Electrical Equipment	Radioactive/Hazardous Materials
___ beamline magnets ___ analysis magnets ✓ target ___ drift chambers ___ other	___ cryo/electrical devices ___ capacitor banks ___ high voltage ___ exposed equipment	List any radioactive or hazadorous/ toxic materials planned for use: ___ ___
Pressure Vessels ___ inside diameter ___ operating pressure ___ window material ___ window thickness	**Flammable Gas or Liquids** (incl. target) type: ___ flow rate: ___ capacity: ___	**Other Target Materials** ___ Beryllium (Be) ___ Lithium (Li) ___ Mercury (Hg) ___ Lead (Pb) ___ Tungsten (W) ___ Uranium (U) ___ Other (list below) ___ ___
Vacuum Vessels ___ inside diameter ___ operating pressure ___ window material ___ window thickness	**Radioactive Sources** ___ permanent installation ___ temporary use type: ___ strength: ___	**Large Mech. Structure/System** ___ lifting devices ___ motion controllers ___ scaffolding or elevated platforms ___ other
Lasers type: ___ wattage: ___ class: ___ **Installation** ___ permanent ___ temporary **Use** ___ calibration ___ alignment	**Hazardous Materials** ___ cyanide plating materials ___ scintillation oil (from) ___ PCBs ___ methane ___ TMAE ___ TEA ___ photographic developers ___ other (list below) ___ ___ ___	**Notes:** ___ ___ ___ ___ ___ ___

CEBAF EXPERIMENT MAJOR REQUIREMENTS

Beam Time (Days)	22
Beam Energies (GeV)	2.4, 3.2, 3.5, 4.0
Beam Type	Unpolarized
Beam Current	$\leq 50\ \mu A$
Targets Needed	Liquid H_2
Power Deposition	≤ 50 watts

BEAM TIME REQUEST

	TIME (DAYS)
Data Acquisition	16.5
Setup and Checkout	1.5
Angle & Energy Changes	0.5
Background Studies	1.5
Contingency (10%)	2.0
TOTAL	22.0

SPECTROMETER REQUIREMENTS

	Electron Arm	Hadron Arm
Solid Angle	5 msr	4 msr
Momentum Acceptance	20%	40%
Momentum Resolution	$\leq 10^{-3}$	$\leq 10^{-3}$
Min Scatt Angle	14.5	13.4
Max Scatt Angle	61.4	23.6
Min Central Momentum	0.7 GeV	1.0 GeV
Max Central Momentum	2.4 GeV	1.7 GeV
Particle i.d. Required	π^-/e^-	π^+/K^+, p/K^+
Required Ratio	0.01	0.005

Longitudinal and Transverse Cross Sections in the d(e,e'K^+)YN Reactions at $Q^2 = 0.5$ to 2 $(GeV/c)^2$

Shelton Beedoe (Spokesman), O. K. Baker* (Co-spokesman), K. Beard, W. W. Buck*, T. Eden, R. Madey†, K. M. Maung, L. Tang*, R. A. Williams
Physics Department, Hampton University
* *and jointly, Physics Division, CEBAF*
† *and Department of Physics, Kent State University*

C. C. Chang, P. Markowitz (Co-spokesman)
Department of Physics and Astronomy, University of Maryland

D. Abbott, L. Cardman, R. Carlini, Y. Chen, R. Ent, S. Majewski, J. Mitchell, W. Vulcan, S. Wood
Physics Division, CEBAF

B. Zeidman
Physics Division, Argonne National Laboratory

E. Hungerford, K. Lan, B. Mayes
Physics Department, University of Houston

J. Napolitano
Department of Physics, Rensselaer Polytechnic Institute

A. Abokar, S. Danagoulian, S. Mtingwa
Physics Department, North Carolina A & T State University

T. Angelescu, A. Mihul
Bucharest University, Bucharest, Romania

F. Garibald, M. Iodice, S. Frullani, E. Cisbani, G. M. URcivoli, R. De Leo, G. Lolos, R. Perrino, T. Leone
INFN, Rome

Abstract

In the one-photon exchange approximation the cross section for the electroproduction reaction d(e, e′K$^+$)YN, where Y is either Λ, Σ^0 or Σ^- and N is a neutron or proton, is a function of contributions from four response functions when both target and incident beam are unpolarized. These cross sections are due to transverse and longitudinal photons, and interference contributions. All four terms in the cross section can in principle be separated over the range of kinematic variables presented in this proposal. This experiment will seek to separate these four cross sections, with particular emphasis on the longitudinal and transverse cross sections by varying the polarization of the virtual photon exchanged between the incoming electron and the target nucleon, while keeping the other relevant quantities fixed. When this separation is achieved, several physics issues can be studied in ways not feasible previously. These include, for example: (i) A comparison of the elementary (e, e′K$^+$) amplitudes between proton and deuteron targets; in addition, the n(e, e′K$^+$)Σ^- reaction will be examined. (ii) A detailed study of the t-channel contributions to the cross sections from a deuteron target. (iii) A study of the ratio of the transverse and longitudinal cross sections to explore possible nuclear effects and constituent quark contributions on the simplest nuclear system before undertaking a study on a heavier nuclei. (iv) A determination of the kaon electromagnetic form factor from a deuteron target. The virtue of this experiment is that the deuteron target is the simplest neutron target, and the simplest nucleus, to study possible Λ-n interactions and modification to the elementary amplitude for the isolated proton. These results (from kaon electroproduction and the L/T separation on the deuteron) will form the basis for a systematic study which will be extended to heavier nuclei and higher energies. The kinematic range for this proposed experiment will cover the electron squared four-momentum transfer from 0.5 to 2 (GeV/c)^2. The High-Momentum Spectrometer (HMS) and Short-Orbit Spectrometer (SOS) in Hall C will be used to measure the scattered electron and hadron momenta, respectively. The kinematic settings will be exactly the same as those already presented in the approved CEBAF experiment 93-018.

1. Introduction

One of the frontier areas of experimental intermediate-energy nuclear physics research is the study of nucleons and nuclear systems with strangeness degrees of freedom. Kaon electroproduction is one example of such a study. Exciting prospects for investigating this process exist at the Continuous Electron Beam Accelerator Facility (CEBAF).

Hadronic-electroproduction reactions can serve as a means of studying hadronic structure via extracted form factors. The understanding of hadronic structure is one of fundamental importance in nuclear and high energy physics. Measuring the elementary amplitudes for K^+ electroproduction on the neutron will provide data on hadronic coupling; furthermore, by studying strange meson production from the nucleon (either proton or neutron), one can in principle deduce the strange quark density inside the nucleon.

In general, QCD has been successful as a theory that describes the strong interactions. At high energies and at large momentum transfers (deep inelastic scattering region), the use of asymptotic freedom allows the application of perturbation theory to describe the structure and interactions of hadrons. At CEBAF energies, one probes the so called transition region from the non-perturbative confinement region to the region of asymptotic freedom. Here, one resorts to phenomenological models in order to describe the strong hadronic interactions because the non-perturbative region of QCD is not well understood. The electromagnetic properties of hadrons can further serve to illuminate models for describing the strong interaction[1, 2, 3].

The proposed experiment will perform detailed separations of the four cross sections, with particular emphasis on the transverse and longitudinal cross sections, σ_U, and σ_L in the reaction

$$e + d \rightarrow e' + K^+ + YN \tag{1.1}$$

where Y is either a Λ, Σ^0 or Σ^- hyperon and N is the associated spectator nucleon, see Fig. 1.1. The kinematic settings will be exactly the same as those already presented in the

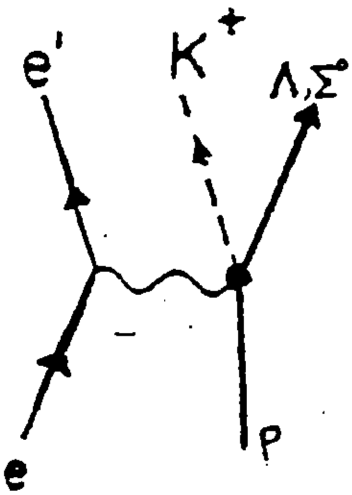

Figure 1.1: Feynman diagram for the electroproduction reaction $^d(e, e'K^+)YN$, where Y is either Λ, Σ^0, *or* Σ^-. Assuming one-photon exchange approximation this is written as $\gamma_v + d \rightarrow K^+ + \Lambda, \Sigma$.

approved CEBAF experiment 93-018[4]. This will further enhance identifying the contributions from the neutron.

In the next section we begin with an overview of hadronic-electroproduction, followed by physics motivations. The experimental set up is presented in the last chapter, along with discussions of background and Monte Carlo, followed by the beam time request.

2. Overview of Mesons Electroproduction

The reaction

$$e + A \rightarrow e' + K^+ + Y + (A - 1) \tag{2.1}$$

forms the basic reaction for the hadron electroproduction off a nuclear target. In the above reaction Y is either a , Σ^0 or Σ^- hyperon and (A-1) represents the remaining nucleons. For A = 1 and assuming one-photon exchange, this can be written as

$$\begin{aligned} \gamma_v + p &\rightarrow K^+ + \Lambda, \Sigma^0 \\ \gamma_v + n &\rightarrow K^+ + \Sigma^- \end{aligned} \tag{2.2}$$

in which the exchanged virtual photon's mass is the squared four-momentum transfer to the target nucleon. The residual baryon Λ, Σ^0 or Σ^- can be identified by its missing mass M_m, given by

$$M_m^2 = (e - e' + p - K)^2. \tag{2.3}$$

Other Lorentz invariant quantities for the kinematics are defined by

$$\begin{aligned} \gamma_v^2 &= (k - k')^2 = q^2 \\ s &= W^2 = (\gamma_v + p)^2 \\ -t &= (\gamma_v - K)^2 \\ Q^2 &= -q^2 \end{aligned} \tag{2.4}$$

where the four momenta are $k = (E, \mathbf{k})$, $k' = (E', \mathbf{k}')$, $K = (\omega, \mathbf{K})$ and $q = (\nu, \mathbf{q})$ for the incident electron, scattered electron, ejected kaon and virtual photon respectively; p is the target nucleon four momentum, and $\nu = E - E'$ is the energy of the virtual photon. If the nucleon is bound within the nucleus, then it can be considered as a virtual (off mass-shell) nucleon and $p^2 \neq M_N^2$.

The kinematics variables and the reaction planes are shown in Fig. 2.1. The angle between

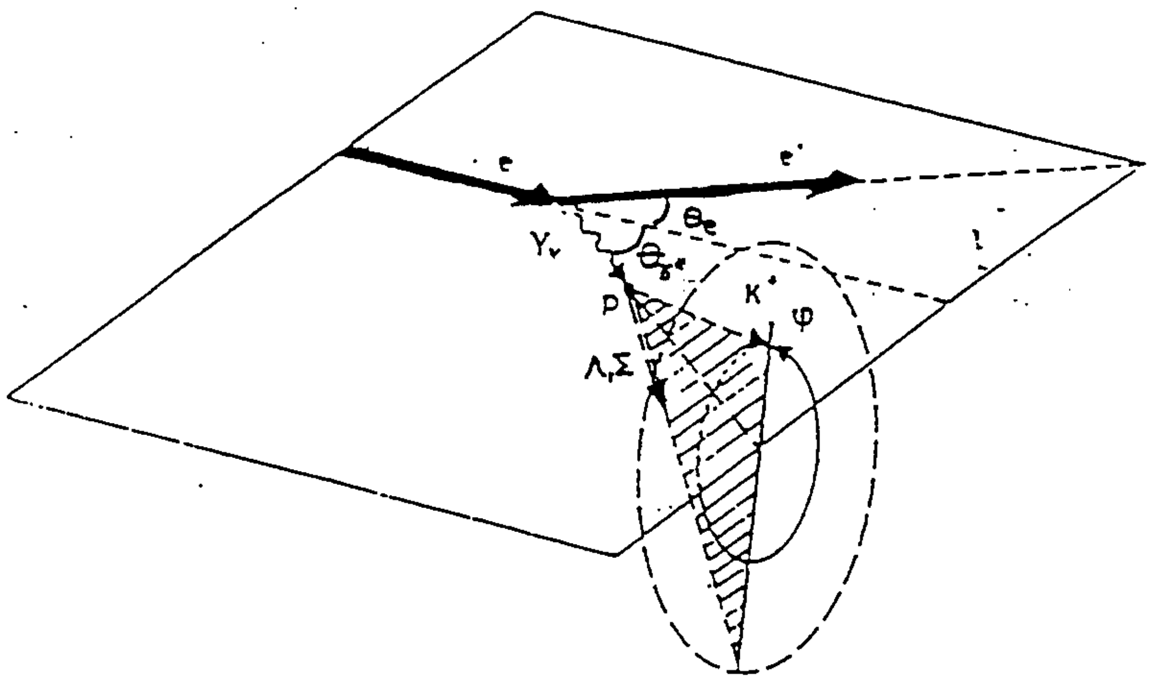

Figure 2.1: **Definition of scattering planes for electrons (initial and final), and ejectiles (kaon and residual particles).**

the initial and scattered electrons is denoted by θ_e. The symbol ϕ_h is the angle between the plane containing initial, final electron momenta and the exchanged photon and the plane containing the ejected kaon and the associated Λ or Σ particle in the final state.

The cross section for the reaction in Eq. (2.2) can be expressed as[5, 6]

$$\frac{d^4\sigma}{dQ^2 ds dt d\phi} = 2\pi\Gamma \frac{d^2\sigma}{dt d\phi}. \tag{2.5}$$

The virtual photon flux Γ is given by

$$\Gamma = \frac{\alpha(s - M^2)}{(4\pi)^2 E^2 M^2 Q^2} \frac{1}{1 - \epsilon} \tag{2.6}$$

and

$$\frac{d^2\sigma}{dtd\phi} = \frac{d\sigma_U}{dt} + \epsilon\frac{d\sigma_L}{dt} + \epsilon\frac{d\sigma_P}{dt}\cos 2\phi + \sqrt{\frac{1}{2}\epsilon(\epsilon+1)}\frac{d\sigma_I}{dt}\cos\phi \tag{2.7}$$

is the single hadron production cross section by virtual photons. The cross sections σ_U and σ_L are the components from photons with their electric vector perpendicular or parallel to the hadronic current 3-vector, i.e., transverse and longitudinal photons. The cross section σ_P represents the interference contributions from the transverse component of the virtual photon and σ_I is due to interference between the transverse and longitudinal components of the virtual photon. The parameter ϵ, $(0 \leq \epsilon \leq 1)$, denotes the degree of polarization of the virtual photon. It is expressed in terms of incident and final electron kinematics as

$$\epsilon = \left[1 + 2\left(1 + \frac{\nu^2}{Q^2}\right)\tan^2(\theta_e/2)\right]^{-1}. \tag{2.8}$$

The separation of the four structure functions would require measurement of the ϵ- and ϕ- dependence of the kaon electroproduction reaction. However the last two ϕ dependent terms can be eliminated by a proper choice of spectrometer settings. By varying ϵ, the remaining first two terms can be separated readily. This makes it feasible to apply a Chew-Low extrapolation method to extract the kaon electromagnetic form factor[6, 7]. The response functions in equation (2.7) are functions of (W^2, Q^2, t). Pion electroproduction data show a decreasing dependence of σ_L on $|t|$[8]. This is expected for kaon electroproduction as well, where σ_L dominates at low t over the remaining three cross sections.

3. Motivation

Already, several approved CEBAF experiments aim to study the elementary amplitudes in the reaction $p(e,e'K^+)Y$, where Y is either a Λ or Σ^0 hyperon[4]. This present proposal is to study the reaction $d(e,e'K^+)YN$ where Y is either a Λ, Σ^0 or Σ^- hyperon and N is the associated spectator nucleon. The emphasis will be on performing detailed longitudinal and transverse (L/T) separation with the deuteron target, varying the virtual photon polarization parameter. With the deuteron target, the reaction (1.1) can be decoupled into the three possible reactions, shown in Eq. (2.2,

$$\mathrm{e} + \mathrm{p} \rightarrow \mathrm{e}' + \mathrm{K}^+ + \Lambda \tag{3.1}$$

$$\mathrm{e} + \mathrm{p} \rightarrow \mathrm{e}' + \mathrm{K}^+ + \Sigma^0 \tag{3.2}$$

$$\mathrm{e} + \mathrm{n} \rightarrow \mathrm{e}' + \mathrm{K}^+ + \Sigma^- \tag{3.3}$$

where the scattered electron and the electroproduced kaon will be detected in the final state.

Most of the past experimental work in electromagnetic production of strangeness on heavy nuclear systems (where heavy means nuclear mass ≥ 2) has concentrated on looking for bound hypernuclear states[9, 10, 11]. By contrast this present program will determine the elementary ($\mathrm{n}(\mathrm{e}, \mathrm{e}'\mathrm{K}^+)\mathrm{Y}$) amplitudes for a neutron target as well as study modifications of the elementary amplitudes ($\mathrm{p}(\mathrm{e}, \mathrm{e}'\mathrm{K}^+)\mathrm{Y}$) for a weakly bound proton. The use of the CEBAF 100-percent duty cycle electron beam will greatly improve the available data[12, 13] for kaon electroproduction on the deuteron and facilitate comparison of the data with theoretical models. The available data exist mostly for the inclusive $\mathrm{d}(\gamma, \mathrm{K}^+)\mathrm{X}$ reaction[14].

For electroproduction on the deuteron system, one should still be able to experimentally separate the Λ and Σ hyperons (by missing mass) assuming that the neutron or proton spectator in the final state has very small initial and final kinetic energy. Previous works indicate that the K^+-n interaction should be small compared to the nucleon-hyperon interaction[9]. Then one can, in principle, isolate the Λ-n interaction.

By separately looking at the reaction in Eq. 3.1 with longitudinal (virtual) photons compared to transverse (virtual) photons, one can hope to disentangle the electromagnetic vertices in Fig. 3.1, just as in the case of a bare proton as presented in CEBAF experiment E93-018[4]. If the electroproduced kaon is detected along the direction of the virtual photon (the forward or **q** direction), then the associated hyperon must be collinear with that kaon s- channel graphs:

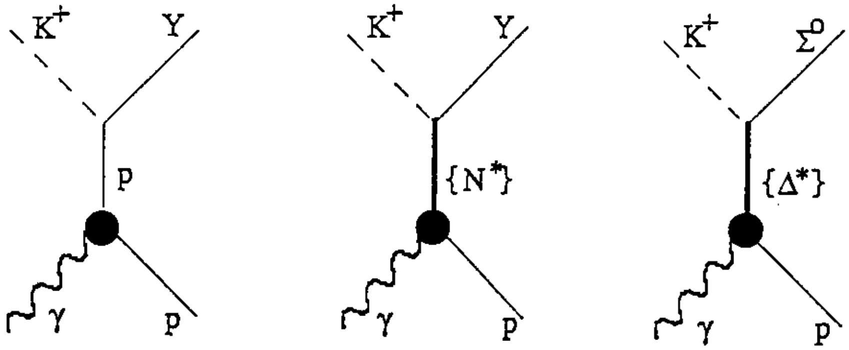

t- channel graphs:

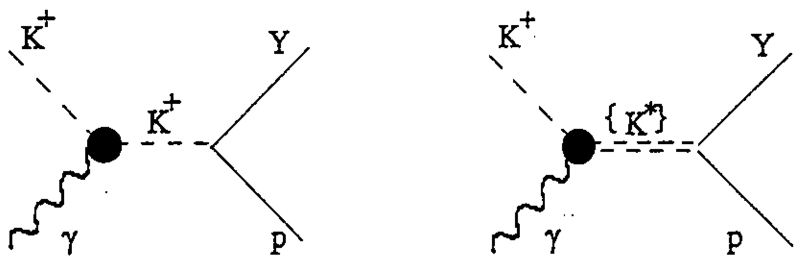

u- channel graphs:

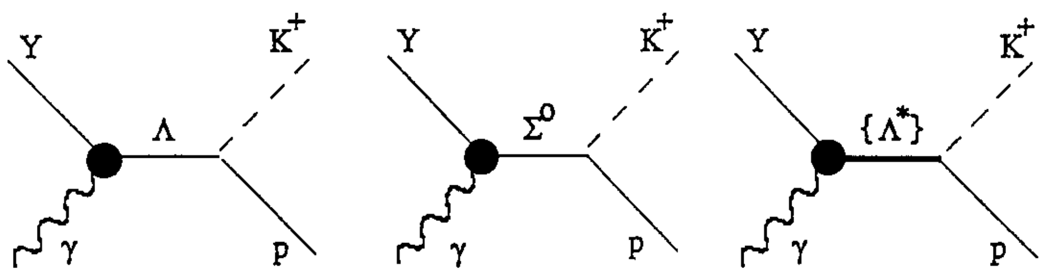

Figure 3.1: Feynman diagram for approximating a one-photon exchange process in the reaction $\gamma_v + \mathrm{d} \to \mathrm{K}^+ + \Lambda$, Σ^0 and $\gamma_v + \mathrm{d} \to \mathrm{K}^+ + \Sigma^-$ by replacing p by n and Λ, Σ^0 by Σ^-.

from simple momentum conservation (if the relative p-n momentum is small in the initial deuteron), additionally, angular momentum conservation selects specific multipole transitions corresponding to the relative K-Y partial waves, i.e., there is a mapping from multipole amplitudes to partial wave amplitudes. By looking at the separate electroproduction cross sections from longitudinal versus transverse photons off a deuteron, one gets, in principle, information on the Λ-n interaction which experiments on the proton can not obtain. The relevant coupling constants $g_{KN\Lambda}$ and $g_{KN\Sigma}$ should be sensitive to whether one observes the longitudinal or transverse cross section. An example of this behaviour is shown in Fig. 3.2, where the cross section is plotted versus Q^2 for the values shown[15, 3].

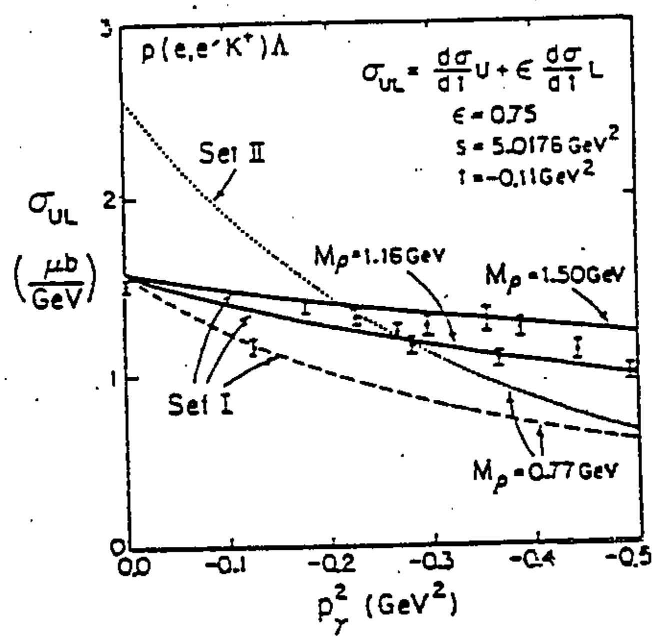

Figure 3.2: Calculated invariant cross section σ_{UL} for p(e, e′K$^+$)Λ at different virtual photon 4-momentum, showing sensitivity to coupling constants[15]. The data are from Ref. [16].

3.1 Separation of the longitudinal and transverse cross sections

The aim of this experiment is to perform a detailed study of the longitudinal and transverse cross sections. The SOS (the hadron arm) will be placed such that, upon averaging, the ϕ-dependent terms can be eliminated. We can easily then separate σ_L from σ_U by a Rosenbluth separation. In this case, with deuteron system, attention should be paid to the hyperon interaction with the nuclear medium and its relevant effect on kaon electroproduction from an off-shell nucleon.

3.1.1 Longitudinal cross section and the t-channel

One can study the t-dependence of the electroproduction process to isolate the t-channel exchange contribution and extract the kaon electromagnetic form factor ($F^D_K(Q^2)$) at high Q^2 in the deuteron system, similarly to the study on the bare proton ($F^p_K(Q^2)$) (using the Chew-Low extrapolation technique). Because the reaction shown in equation (1.1) should be independent of whether the reaction takes place on a nucleon or in a nucleus (if the spectator approximation is valid), one expects the ratio $F^D_K(Q^2)/F^p_K(Q^2)$ to be unity at all values of the momentum transfer squared. Any deviations from this result would signal a modification of the kaon electromagnetic structure due to either the nuclear binding (i.e. an off-shell nucleon) or the Λ-n FSI. The virtue of the deuteron target is that it provides the simplest nucleus for studying differences with respect to elementary electroproduction.

In the t-channel the virtual photon directly couples to the kaon. Only longitudinally polarized photons will scatter in the forward direction from the kaon (or mesonic current of the nucleon) in the t-channel; and the kaon form factor is thus extracted from the longitudinal component. This contribution is enhanced when the variable $|t|$ is at a minimum, which depends on the squared virtual photon mass as shown in Fig. 3.3. Some of the possible sources of kaons are indicated in Fig. 3.1. In Fig. 3.1b the virtual photon couples to a virtual

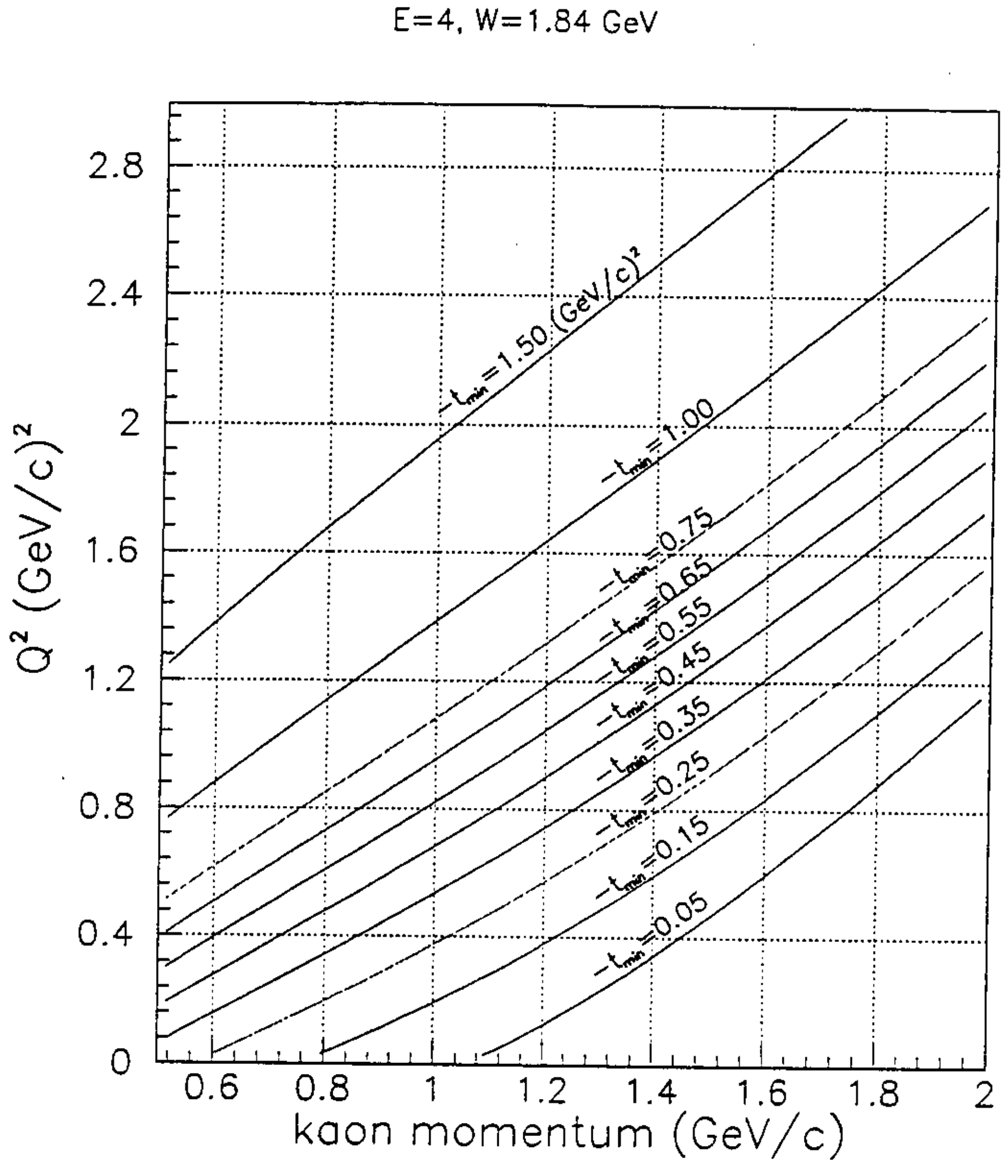

Figure 3.3: **The variable t_{min} dependence on (Q^2, p_K), p_K = kaon momentum.**

kaon emitted by the target nucleon. Most of the physics discussed here will seek to separate out the t-channel K^+ production mechanism from the other possibilities because this is the relevant mode which involves the kaon electromagnetic form factor—it is the Born term in the t-channel. The s- and u-channel Born terms are shown in Fig. 3.1. Replacing p by n, and replacing Λ and Σ^0 by Σ^-, will give similar diagrams for the neutron. Higher-order contributions are not indicated, but their contributions are worth consideration.

The pion electromagnetic form factor has been extracted using the longitudinal component of the electroproduction cross section, σ_L. The t-dependence of σ_L allows one to extract the kaon form factor in a parallel fashion as that for the pion. The method generally used is the Chew-Low extrapolation technique[6, 7]. The contribution due to the pole term is parameterized as[7]

$$\sigma_L \propto -tF_\pi^2(Q^2,t)\frac{g_{\pi NN}^2(t)}{(t-m_\pi^2)^2} \tag{3.4}$$

for the pion pole. Following the prescription set above for pion, the kaon pole contribution can similarly be expressed as

$$\sigma_L \propto (-t+(M_p-M_\Lambda)^2)F_K^2(Q^2,t)\frac{g_{KN\Lambda}^2(t)}{(t-M_K^2)^2} \tag{3.5}$$

where t is the squared four-momentum transfer, $g_{\pi NN}(t) = g_{\pi NN}(0)(1-t/\Lambda_{\pi N}^2)^{-}1$ is the πNN vertex form factor[17], and $(g_{KN\Lambda})$ is the coupling to the $(KN\Lambda)$ vertex. Model calculations done by C. Ji and S. Cotanch, utilizing a vector meson dominance model, in which the virtual photon couples to a ρ or ϕ meson, and a QCD type calculation are compared to the $p(e,e'K^+)$ data[18]. There is reasonable agreement at low Q^2.

3.1.2 Transverse cross section

The electroproduction of pseudoscalar mesons by transversely polarized virtual photons has been examined in the quark-parton model[19]. Looking at the s-channel, it was found that for scattering followed by hadronization by vector gluons, the transverse-transverse interference part of the cross section, σ_P, is strictly zero, and the part of cross section due to transversely polarized photons, σ_U, has the relative behavior as a function of t shown in Fig. 3.4a. In scattering by a transversely polarized virtual photon followed by hadronization by a scalar gluon, it was found that the transverse-transverse interference piece, σ_P, is not equal to zero, and the behavior of the transverse cross section σ_U is given as a function of t by Fig. 3.4b, due to helicity conservation.

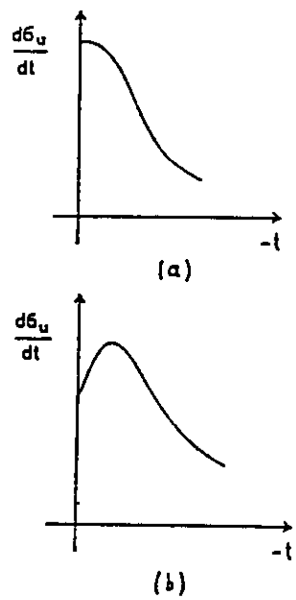

Figure 3.4: Transverse cross section vs t for (a) exchange of vector gluons, or (b) scalar gluons.

An example of this model can be found in the pion electroproduction data[5], where the ratio of π^+ electroproduction from the proton to π^- electroproduction on the neutron was measured. The proton is described in terms of the valence quarks uud (charge 2/3, 2/3, -1/3) while the neutron is described as udd (charge 2/3, -1/3, -1/3). The π^+ (π^-) is a $\overline{u}d$ ($\overline{d}u$), meaning that for π^+ electroproduction, the virtual photon couples to the valence u quark, with charge 2/3. However for π^- electroproduction, the virtual photon couples to the valence d quark, with charge -1/3. The ratio of π^+ to π^- electroproduction should be $|2/3|^2 : |-1/3|^2 = 4:1$. As seen in Fig. 3.5, the data[5] approach 4:1 as as |t| increases.

It is worth asking why this behavior should be seen as a function of t, which is after

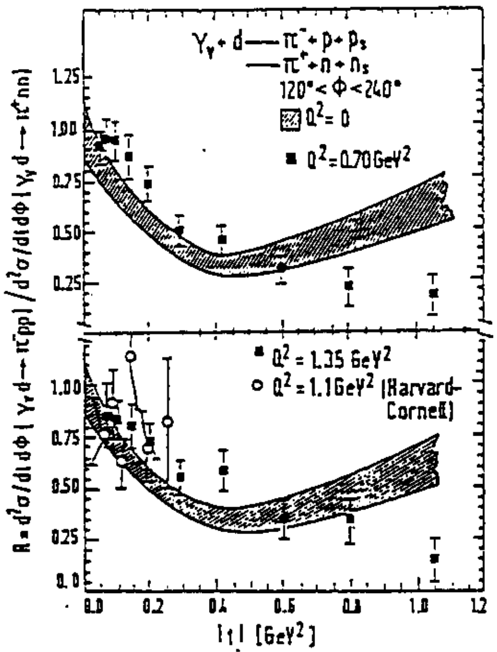

Figure 3.5: The ratio of π^- to π^+ production off deuterium including data at $Q^2 = 0$ [5].

all inherently an exclusive quantity. The data shown are the cross section data, where no L/T separation was performed. This means that as the absolute value of t increases, the longitudinal piece of the cross section dies away, leaving just the transverse piece showing the expected behavior. This experiment will measure the behavior of the separated L/T responses as a function of both t and Q^2 to map out the behavior.

It is also worth asking whether or not this behavior is observed with real photons. The cross section for real photons is all transverse, and one might expect the photoproduction cross section to also show this behavior; it does not. For real photons $Q^2 = 0$ and $x_{Bj} = Q^2/2M\nu = 0$. The valence quark structure functions quarks peak at roughly $x_{Bj} = 0.3$, whereas the sea quarks peak at $x_{Bj} = 0$, and fall away to essentially zero by $x_{Bj} = 0.2$ [20, 21]. Therefore real photons preferentially see the sea quarks, not the valence quarks. This experiment will measure between $0.2 \leq x_{Bj} \leq 0.5$, where scattering from valence quarks should dominate.

The analogy between π^+/π^- (or $u\bar{d}/d\bar{u}$) to the case of kaons is the K^+/K^0 ratio (or $u\bar{s}/d\bar{s}$). The quark-parton model predicts that the ratio of the transverse cross section for

$K^+\Sigma^0$ production on the proton to $K^+\Sigma^-$ production on the neutron is[19] 1:2 reflecting the probability of finding the ud quarks in the proton in a I=1 state compared to the probability of finding the dd quarks in the neutron in a I=1 state. The important point here is that it is necessary to do an L/T separation to see the behavior of σ_U, the transverse part of the cross section.

There is also a perturbative QCD (pQCD) prediction[22] for photoproduction of kaons. The calculation is the leading twist, Born approximation helicity amplitudes for s-channel scattering from valence quarks. Shown in Fig. 3.6, the cross section is plotted as a function

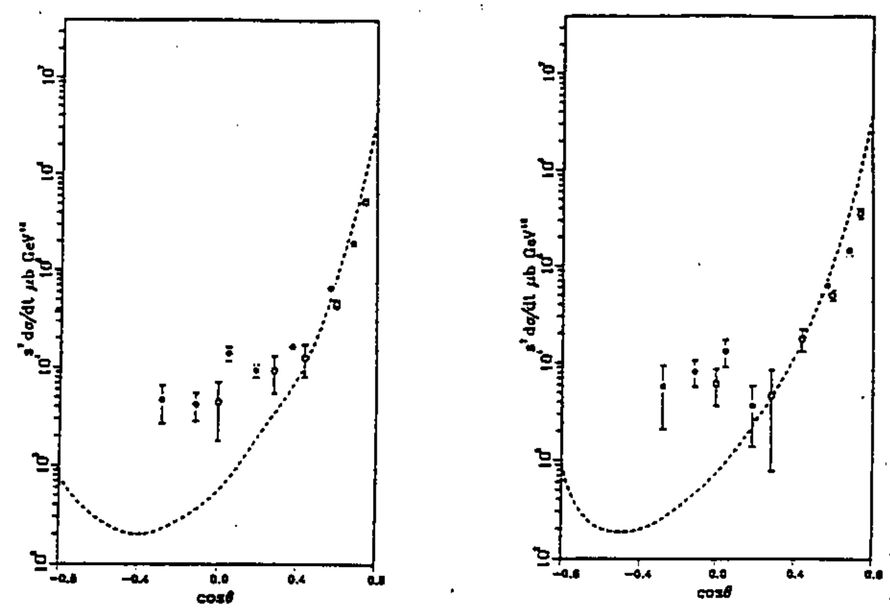

Figure 3.6: **Unpolarized cross section $s^7 d\sigma/dt$ with $\epsilon = 0.01$, for $\gamma p \to K^+\Lambda^0$ (left) and $\gamma p \to K^+\Sigma^0$ (right)[22] compared to the data[23] for 4 (6) GeV, solid (open) circle.**

of $\cos\theta$, where θ is the angle between the photon and the outgoing kaon (this is equivalent to t). The calculation is sensitive to the quark wave functions, which give a different behavior for the Λ channel versus the Σ channel (the dip for the Λ occurs around $\cos\theta = -0.5$, while the dip for the Σ occurs around $\cos(\theta) = -0.5$.) As can be seen, the photoproduction data are not in perfect agreement with the calculation. At forward angles, the t-channel contributes, while at backward angles the u-channel contributes. This prediction should hold more rigorously for the transverse part of the electroproduction cross section for the reasons given above ($0.2 \leq x_{Bj} \leq 0.5$ allows one to scatter predominantly from a valence quark, the L/T separation allows one to minimize the t-channel contribution, and the t-behavior will be mapped out by changing the kaon angle while keeping the electron arm fixed).

3.2 $(K^+, \Sigma^0)/(K^+, \Lambda)$ ratio

The ratio $(K^+, \Sigma^0)/(K^+, \Lambda)$ has interesting physical meanings. It is conjectured that the (K^+, Σ^0) cross section falls faster with Q^2 than the cross section from (K^+, Λ). One argument in favor of this is that the coupling constant [5] $g^2_{pK\Lambda} \gg g^2_{pK\Sigma^0}$. There are other arguments which are also presented in Refs. [24,25]. These scenarios presented can be further understood when data are available for separated cross sections. Importantly, it is the σ_L dominance that explains the observed decreasing ratio [5, 26, 27] in the experimental data. The Q^2 dependence of

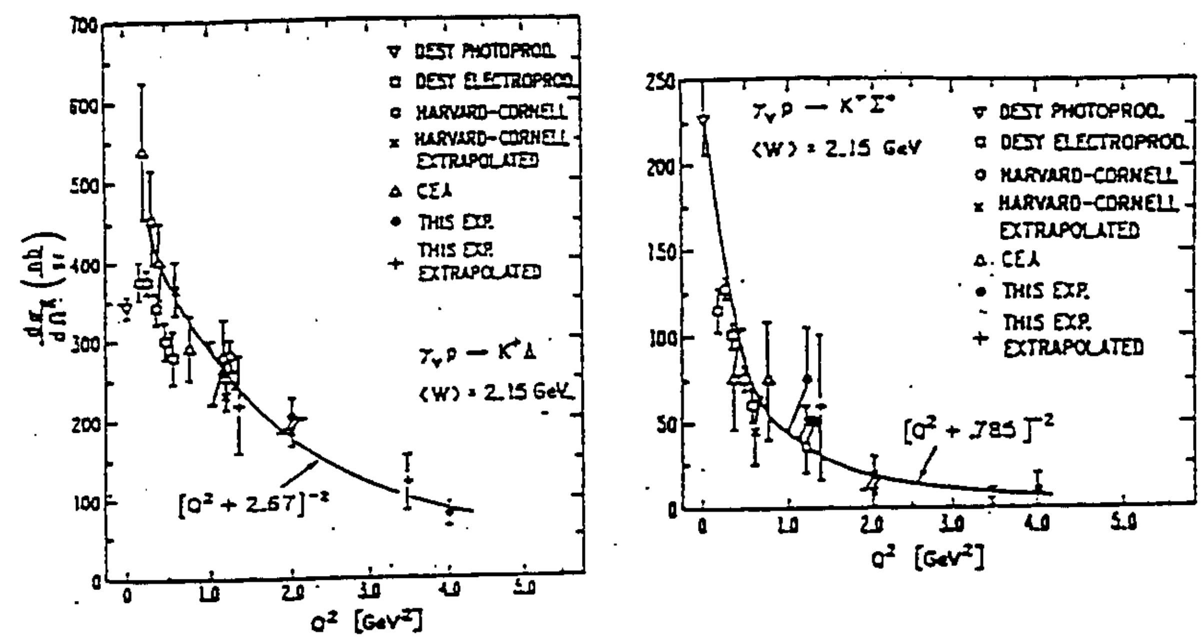

Figure 3.7: The Q^2 dependence of kaon electroproduction cross section for the case in which there is Λ or Σ particle in the final state[5]. Similar study will be done for as proposed on the deuteron.

interesting is the high statistics experiment to study this dependence for the nuclear target as proposed here. The effect of the multi-nucleon environment can be inferred from these data and the effective physical coupling constants in the presence of FSI's can be determined. The study on the deuteron is the beginning of a systematic study which will be extended to heavier systems where these effects are expected to be large.

4. Experimental Procedure

4.1 Experimental arrangements and kinematics

The data on the above targets will be obtained with the apparatus in experimental Hall C at CEBAF. For this measurement, the two spectrometers needed are the High Momentum Spectrometer (HMS) and the Short Orbit Spectrometer (SOS). A plan view of Hall C is shown in Fig. 4.1. The momentum of the final scattered electron is measured by utilizing the HMS and the produced meson is observed in the SOS. For the HMS arm, the detector stack follows three quadrupole magnets and one dipole magnet. Similarly, the SOS arm will contain one quadrupole magnet and two dipole magnets bending in opposite directions. The proposed detector stacks for the two spectrometers are shown in Fig. 4.2.

The choice of kinematics dictates the spectrometer settings listed in Table 4.1. The total c.m. energy $W = \sqrt{s}$ is chosen here to be above the resonance region. Contours for these kinematic variables are shown in Figs. 4.3.

4.2 Background considerations

On the HMS arm, a gas Čerenkov will be used on-line to reject pions. Further pion rejection will be achieved off-line by utilizing the lead-glass shower counter detector (see Fig. 4.4a).

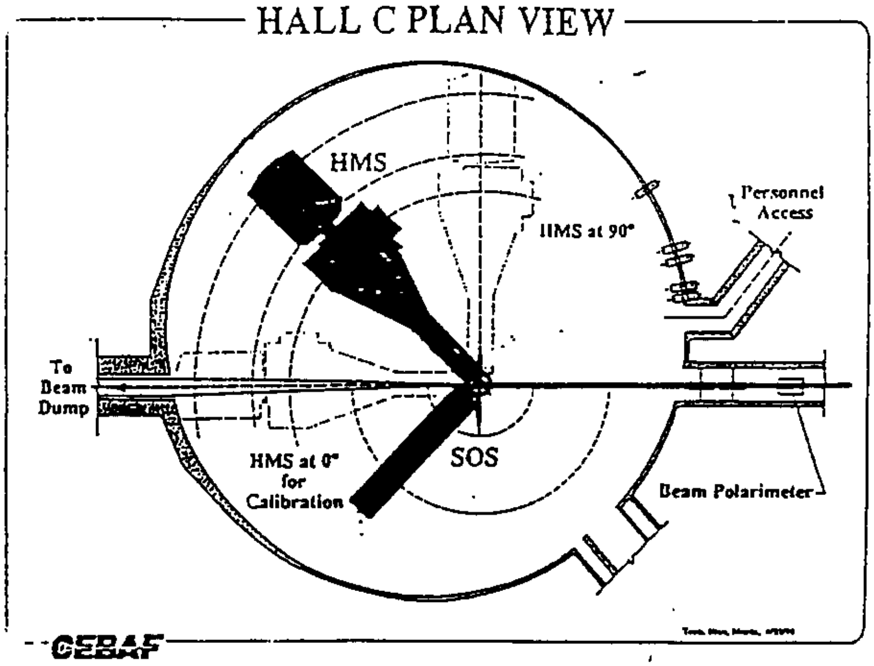

Figure 4.1: Set up of experimental Hall C. The scattered electrons will be detected in the HMS while the kaons will be detected in the SOS.

Kine.	Q^2	E_e	E'_e	θ_e	θ_γ	W	ν	ϵ	x
1a	0.50	2.40	0.80	29.56	13.04	1.84	1.60	0.54	0.17
1b	0.50	3.20	1.57	18.25	16.31	1.84	1.60	0.76	0.17
1c	0.50	4.00	2.39	13.16	18.10	1.84	1.60	0.86	0.17
2a	1.00	2.40	0.61	49.20	12.76	1.81	1.80	0.36	0.30
2b	1.00	3.20	1.38	27.69	18.08	1.81	1.80	0.66	0.30
2c	1.00	4.00	2.19	19.48	20.77	1.81	1.80	0.80	0.30
3a	1.50	2.40	0.61	61.37	12.98	1.69	1.85	0.28	0.43
3b	1.50	3.20	1.34	34.39	19.91	1.69	1.85	0.61	0.43
3c	1.50	2.40	2.23	23.42	23.56	1.69	1.85	0.78	0.43
4a	2.00	3.20	0.79	53.14	13.03	1.84	2.40	0.34	0.44
4b	2.00	3.50	1.09	42.51	15.33	1.84	2.40	0.46	0.44
4c	2.00	4.00	1.59	32.67	17.90	1.84	2.40	0.60	0.44

Table 4.1: Kinematics Settings

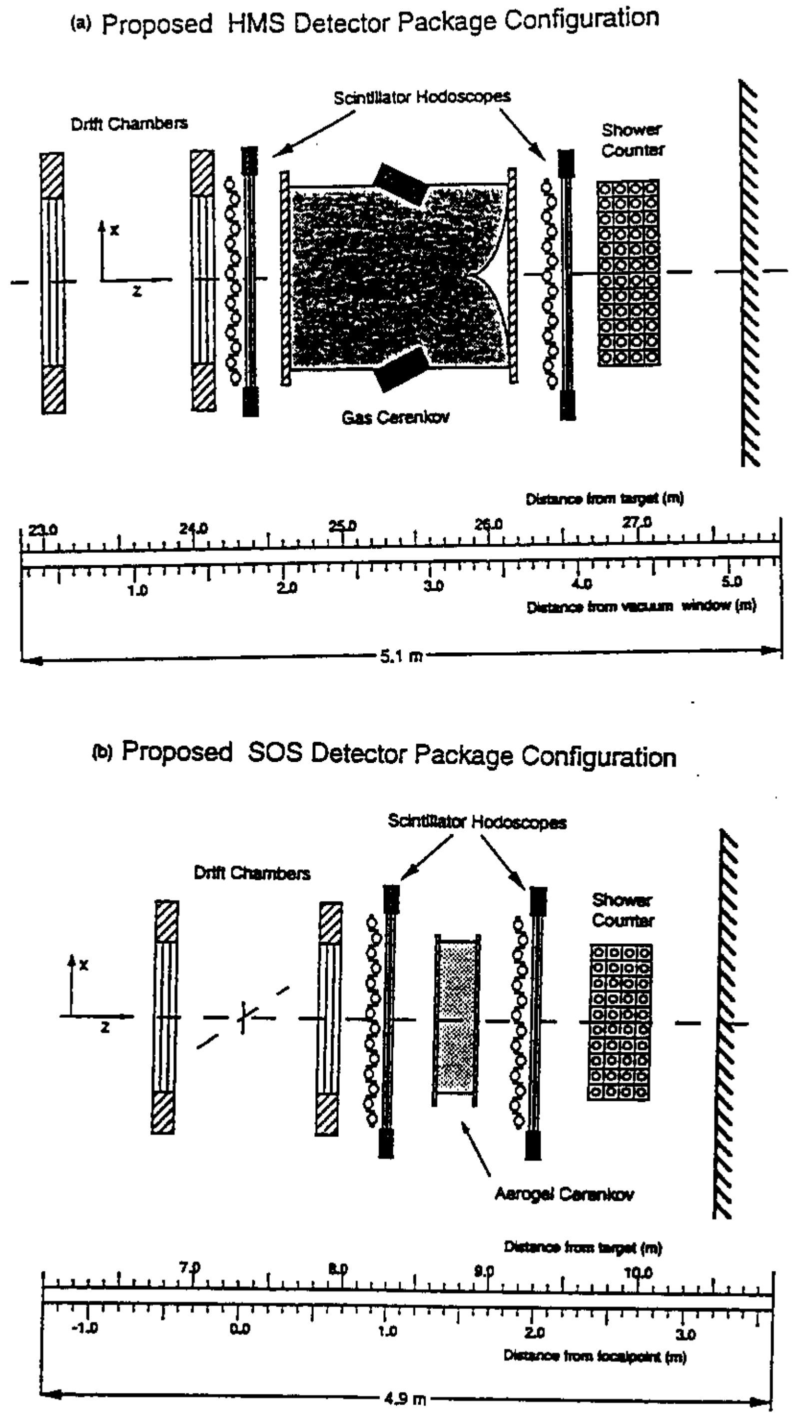

Figure 4.2: (a) HMS detector plan view. (b) SOS detectors plan view.

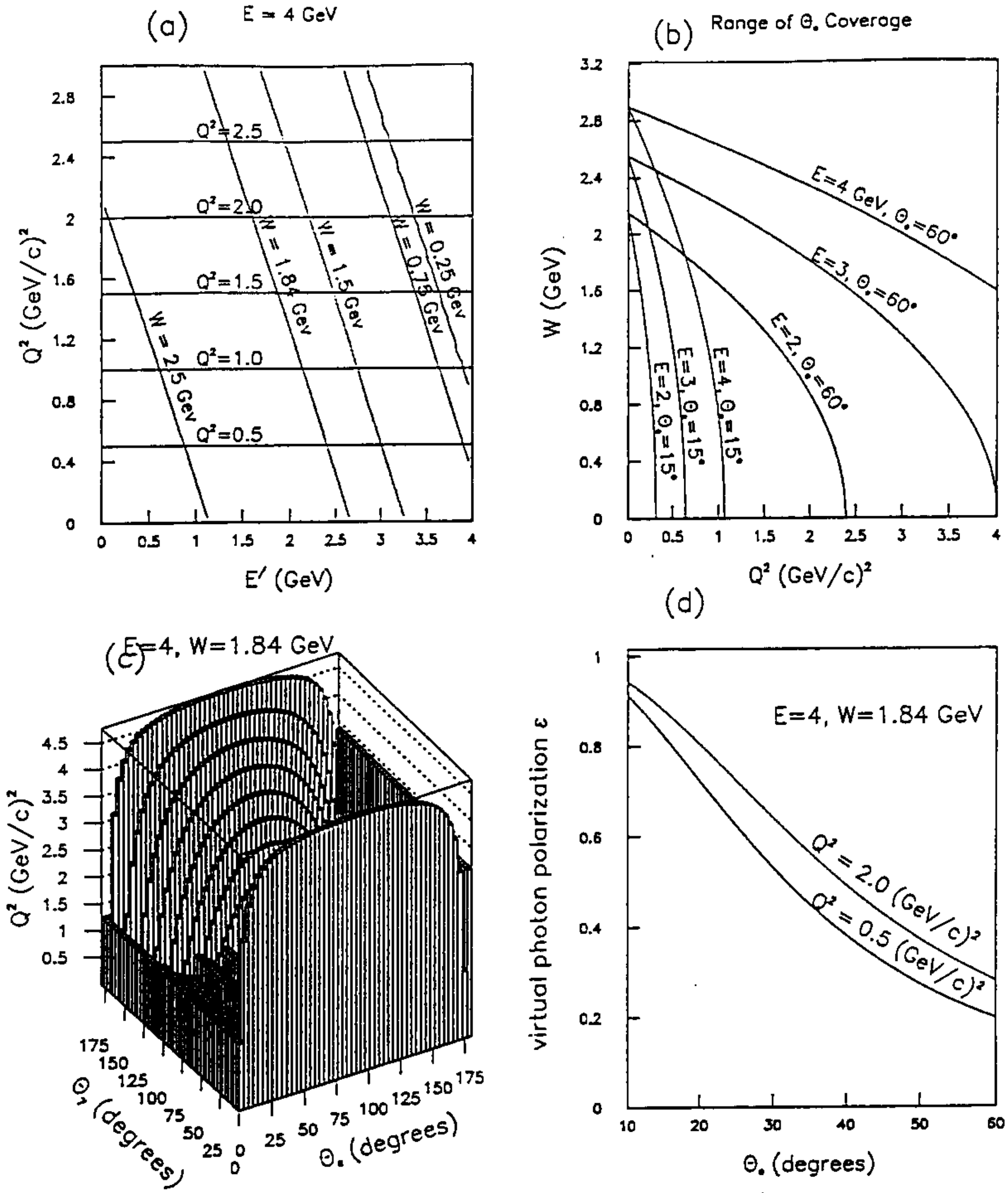

Figure 4.3: Kinematics contours describing available phase space. (a) The W-dependence in the (Q^2, E′) plane. For this experiment, W will vary between 1.7 and 1.9 GeV. (b) Range of coverage for the electron arm in the (W, Q^2) plane. (c) Hypersurface for the dependence of Q^2 on the scattered electron and virtual photon direction over possible combinations. (d) Virtual photon polarization parameter dependence on electron kinematics for the Q^2 and W of this proposal.

The hadron arm will utilize a time-of-flight (TOF), coincidence window on the order of 2 ns off-line and an anti-π coincidence mode trigger of the threshold pion Cerenkov, to reject slow protons and pions. The collaboration is currently investigating the implementation of an H_2O threshold kaon Čerenkov detector[28]. This effort is being undertaken by the North Carolina A&T State University members of the collaboration with Hampton University participating.

4.3 Count rate estimates

We estimate the rates in each detector using the luminosity set forth in the CEBAF Conceptual Design Report (CDR)[29]. The envisioned effective target length is 5 cm and beam currents of 10 to 30 μA. Power dissipation in the target for this current should be minimal. In calculating the rates the laboratory cross section $\frac{d^3\sigma}{dE'_e d\Omega_e d\Omega_K}$ was computed from experimental data (e.g. Refs. [12,30]) extrapolated for other Q^2 and W values. For the singles rates, the eN cross section is written in the Rosenbluth form. The dipole form factor has been used to describe the momentum-transfer dependence. The cross section has been computed both for protons and neutrons and added incoherently, similar to that used in Ref. [31]. The kaon laboratory cross section was integrated over momentum bite of $\pm 0.20 p_0$[32].

In estimating the coincidence rate $R_c(e, e'K)$, we use

$$R_c(e, e'K) = \frac{I}{e} \cdot \frac{\rho t N_0}{A} \cdot \frac{d^3\sigma}{dE_e d\Omega_e d\Omega_K} \cdot \Delta E_e \Delta\Omega_e \Delta\Omega_K \cdot (1 - P_{\mathbf{decay}}) \tag{4.1}$$

with t = 5 cm (target length), $\Delta\Omega_e = 5$ msr, $\Delta\Omega_K = 4$ msr, $\Delta E'_e = 0.2 E'_e$, $\Delta\Omega$ is the solid angle of the spectrometer, and $P_{\mathbf{decay}}$ is the kaon survival probability over a 10 m flight path. The beam currents (I = 10—30 μA) have been chosen to maximize the signal to noise ratio. $R_e(e, e')$ and $R_K(e, K)$ are the singles rates in the HMS and SOS arms respectively. The ratio of accidental to true is

$$\frac{A}{T} = \frac{\tau \cdot R_e \cdot R_K}{f \cdot R_c}$$

where $\tau = 1$ ns resolving time and f = 1 duty factor have been used. The contribution

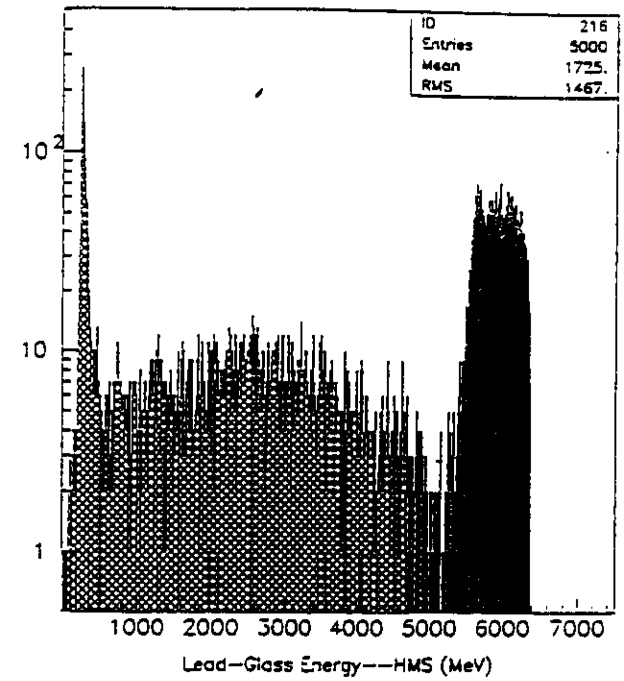

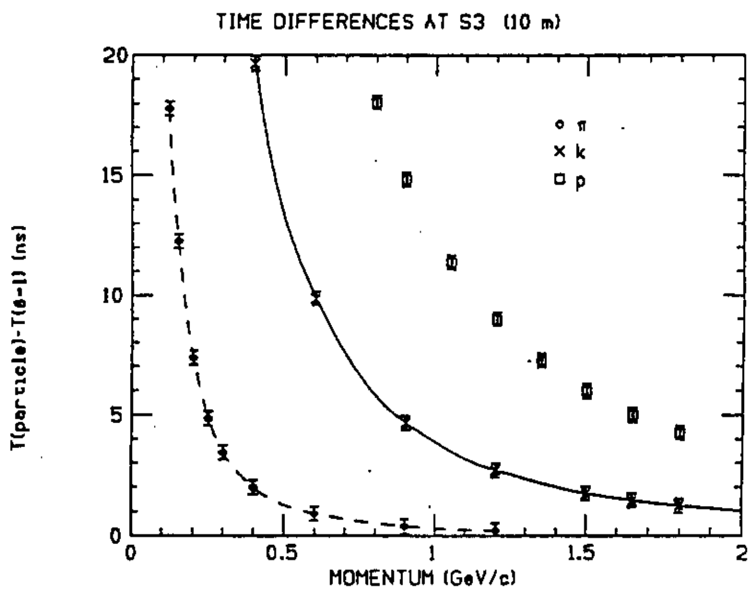

Figure 4.4: A GEANT simulated (a) electron-pion events, generated over a momentum range of 6±.4 GeV/c in the HMS arm, and (b) TOF difference for π, K^+, p separation in the SOS arm over a momentum range of 0.8 to 1.8 GeV/c.

$\sigma(\gamma_v n \rightarrow K^+\Sigma^-)$ for the neutron in deuterium was taken to be the same as $\sigma(\gamma_v p \rightarrow K^+\Sigma^0)$. Table 4.2 lists the computed rates for the kinematics conditions in Table 4.1.

Kine.	I (μA)	R_c(e,e'K) (10^{-2} Hz)	R_e(e,e') (kHz)	R_K(e,K) (kHz)	A/T ($\tau = 1$ ns)
1.a	10	6.50	5.30	1.33	0.11
1.b	10	19.1	24.0	1.22	0.15
1.c	10	38.0	56.5	1.19	0.17
2.a	20	2.14	0.40	3.32	0.06
2.b	20	7.20	2.78	2.70	0.10
2.c	20	15.4	7.50	2.10	0.12
3.a	30	0.56	0.09	2.34	0.04
3.b	30	1.94	0.70	1.90	0.07
3.c	30	4.10	1.97	1.70	0.08
4.a	30	0.94	0.06	8.52	0.05
4.b	30	1.44	0.12	7.45	0.06
4.c	30	2.47	0.28	6.36	0.07

Table 4.2: **Coincidence and single rates for d(e,e'K^+) Λ Σ^0 or Σ^-.**

4.4 GEANT Monte Carlo

Both the HMS and SOS detectors have been simulated in GEANT. With these simulations the systematics can be better understood in a timely manner—an effort that otherwise could cost a considerable amount of beam time. The simulation includes details of the detector geometry and material. The response of the detector elements when particles propagate through the experimental set up are digitized and recoded into appropriate format consistent with the expected CODA data format. This work allows one to develop and test tracking software and study detector resolution. Effects from processes like multiple scattering, particle decay, energy loss, etc. are calculated easily. The energy deposited in the 1-cm scintillator element for (π, K^+, p) is shown in Fig. 4.5.

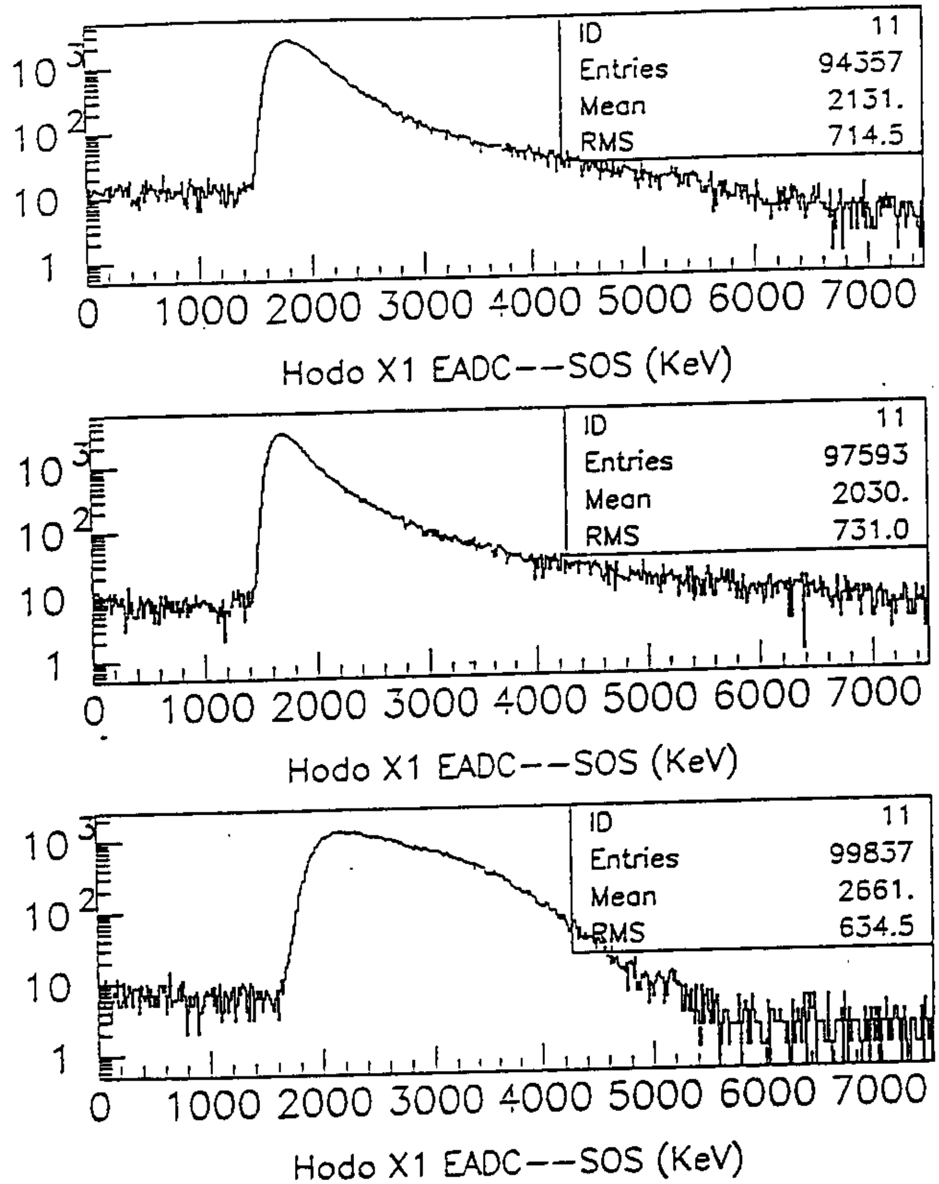

Figure 4.5: The energy deposited in the SOS X1 scintillator array for π (top), K^+ (middle) and proton (bottom). The events were generated over a momentum range of 0.8—1.8 GeV/c.

4.5 Run time and measurement errors

The final real events will contain some background from random coincidence events. Our current estimates are based on statistics. Other sources of background resulting from random coincidence and corrections due to finite detector acceptance will be corrected off-line. Most of the kinematic variables discussed in this proposal that appear in the cross sections given in Eq. 2.7 are functions of Q^2, W, and t. The uncertainties in Q^2 and W are simply due the electron kinematics, i.e., E, E′ and $\theta_{e'}$. The uncertainties in Q^2, W, and t are thus estimated to be less than 1, 5, and 1% respectively. Overall an uncertainty of < 5% is expected for the uncertainty in the cross sections. Fermi momentum smearing of the missing mass will be determined in a Monte Carlo fashion. The GEANT simulation package (which is available presently) will be used to better understand systematics and other sources of errors.

The beam time required to obtain reasonable statistics is summarized in Table 4.3. A total of 22 days of running is requested.

	TIME (DAYS)
Data Acquisition	**16.5**
Setup and Checkout	**1.5**
Angle & Energy Changes	**0.5**
Background Studies	**1.5**
Contingency (10%)	**2.0**
TOTAL	**22.0**

Table 4.3: **Beam Time Request**

References

[1] Joseph Cohen . *Phys. Lett.*, **153B**, 367, 1985.

[2] T. E. Rudy, H. W. Fearing and S. Scherer . *TRI-PP-94-4*, 1994.

[3] Robert A. Williams et al. . *Phys. ReV.*, **C46**, 1617, 1992.

[4] O.K. Baker (Spokesman) . *CEBAF Proposal PR 93-018.*

[5] P. Brauel et al. . *Z. Physik. C, Part. and Fields*, **3**, 101, 1979.

[6] R. C. E. Devenish et al. . *Phys. Rev.*, **D5**, 47, 1972.

[7] W. R. Frazer . *Phys. Rev.*, **115**, 1763, 1959.

[8] P. Brauel et al. . *Phys. Lett.*, **69B**, 253, 1977.

[9] F. M. Renard and Y. Renard . *Phys. Lett.*, **24B**, 159, 1967.

[10] C. B. Dover, D. J. Millener, A. Gal . *Physics Report*, **184**, 1, 1989.

[11] R. S. Hayano . *Nucl. Phys.*, **A527**, 477c, 1991.

[12] C. J. Bebek et al. . *Phys. Rev.*, **D15**, 594, 1977.

[13] A. M. Boyarski et al. . *Phys. Lett.*, **34B**, 547, 1971.

[14] D. J. Quinn et al. . *Phys. Rev.*, **D20**, 1553, 1979.

[15] Shian S. Hsiao and Stephen R. Cotanch . *Phys. Lett.*, **163B**, 300, 1985.

[16] T. Azemoon et al. . *Nucl. Phys.*, **B95**, 77, 1975.

[17] C. E. Carlson and Joseph Milana . *Phys. Rev. Lett.*, **65**, 1717, 1990.

[18] Chueng-Ryong Ji and Stephen R. Cotanch . *Phys. Rev.*, **D41**, 2319, 1990.

[19] O. Nachtmann . *Nucl. Phys.*, **B115**, 61, 1976.

[20] CCFR Collaboration . *Phys. Rev. Lett.*, **64**, 1207, 1990.

[21] H. Deden et al. . *Nucl. Phys.*, **B85**, 269, 1975.

[22] G. R. Farrar et al. . *Nucl. Phys.*, **B349**, 655, 1991.

[23] R. L. Anderson et al. . *Phys. ReV.*, **D14**, 679, 1976.

[24] O. Nachtmann . *Nucl. Phys.*, **B74**, 422, 1974.

[25] J. Cleymans and F. E. Close . *Nucl. Phys.*, **B85**, 429, 1975.

[26] C. J. Bebek et al. . *Phys. Rev. Lett.*, **32**, 21, 1974.

[27] C. J. Bebek et al. . *Phys. Rev.*, **D17**, 1693, 1978.

[28] S. Danagoulian, North Carolina A & T State University (private communications) .

[29] . *CEBAF Conceptual Design Report, (1990).*

[30] C. J. Bebek et al. . *Phys. Rev.*, **D15**, 3082, 1977.

[31] L. W. Lightbody and L. S. O'Connell . *Comp. Phys. May/June*, page 57, 1988.

[32] T. Angelescu, Bucharest University (private communications) .